A Multi-purpose RGB-D Dataset for Understanding Everyday Objects

Shuichi Akizuki and Manabu Hashimoto
Department of Engineering, Chukyo University, Nagoya, Aichi, Japan

Keywords: Dataset Generation, Semantic Segmentation, Affordance, 6DoF Pose Estimation.

Abstract: This paper introduces our ongoing work which is a project of establishing a novel dataset for the benchmarking of multiple robot vision tasks that aims to handle everyday objects. Our dataset is composed of 3D models, RGB-D input scenes and multi-type annotations. The 3D models are full-3D scan data of 100 everyday objects. Input scenes are over 54k RGB-D images that capture the table-top environment, including randomly placed everyday objects. Our dataset also provides four types of annotation: bounding boxes, affordance labels, object class labels, and 6 degrees of freedom (6DoF) poses. These are labeled for all objects in an image. These annotations are easily assigned to images via an original 6DoF annotation tool that has a simple graphical interface. We also report benchmarking results for modern object recognition algorithms.

1 INTRODUCTION

Achieving human-like tool use using robotic arms is one of the important goals for intelligent robotics. Object detection, segmentation and 6 degrees of freedom (6DoF) pose estimation are an effective way to reach this goal. Recent state-of-the-arts deep-learning techniques have been enabled robot arms to accurately recognize and grasp target objects. For example, Single shot multibox detector (SSD) (Liu et al., 2016) can detect multiple objects in real time from RGB images. Dex-Net 4.0 (Mahler et al., 2019) can detect the suitable grasping regions for picking up randomly stacked objects with a reliability greater than 95%.

However, these methods are not enough for human-like tool use. They dont understand the appropriate regions that carry out the specific tasks for tool use. In the case of the object detection, a robot can understand the position of a mug as a bounding box, but it cannot provide information about the region that could contain liquid.

Understanding the affordance (the functionality of a parts shape) is also an effective way to achieve human-like tool use (Do et al., 2018). In the case of a hammer, the grip part can be used to grasp and the head part can be used to pound another object. These parts are used to apply the tasks of grasping and pounding. Affordance estimation is generally treated as the semantic segmentation. However, preparing the training data needs a large amount of time and labor.

In order to solve this problem, we propose a low-cost annotation procedure for multiple tasks including affordance segmentation. And we have developed a novel dataset by using the proposed method. The proposed method enables the annotation of four kinds of information: bounding boxes, 6DoF poses for each object, pixel-wise object class labels, and the affordance label shown in figure 2. To the best of our knowledge, our dataset is the largest that can be evaluated for multiple tasks including affordance segmentation. The dataset can be downloaded from our website [1]. In this paper, we report the benchmark-

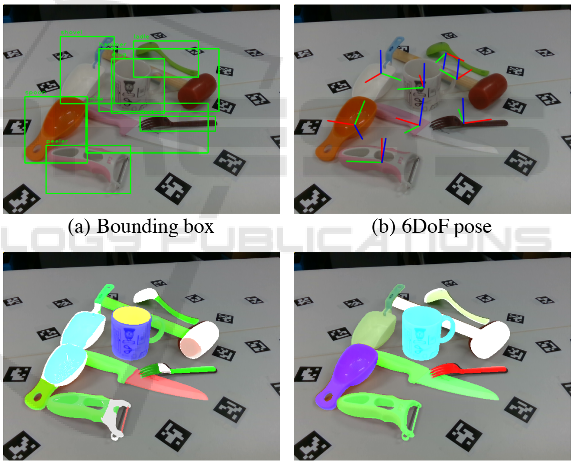
(a) Bounding box
(b) 6DoF pose
(c) Affordance label
(d) Object class label

Figure 1: Multiple annotations provided by proposed dataset.

[1] http://isl.sist.chukyo-u.ac.jp/archives/nedopro/

Akizuki, S. and Hashimoto, M.
A Multi-purpose RGB-D Dataset for Understanding Everyday Objects.
DOI: 10.5220/0009142504700475
In *Proceedings of the 15th International Joint Conference on Computer Vision, Imaging and Computer Graphics Theory and Applications (VISIGRAPP 2020) - Volume 5: VISAPP*, pages 470-475
ISBN: 978-989-758-402-2; ISSN: 2184-4321

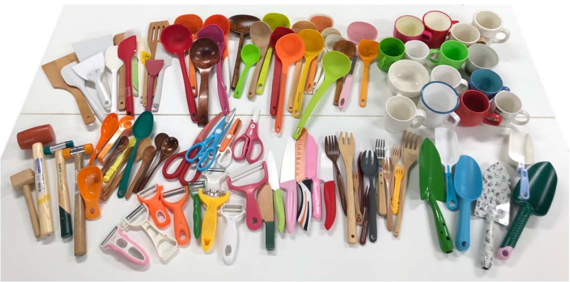

Figure 2: Kitchen and DIY tools.

ing results for object detection and segmentation using modern deep-learning architectures.

Table 1 summarizes the contents of RGB-D datasets that can be used for evaluating multiple tasks. RGB-D Part Affordance Dataset(Myers et al., 2015), IIT-AFF(Do et al., 2018) and NEDO-v1(Akizuki and Hashimoto, 2019) are the datasets for the affordance estimation of tools. They provide pixel-wise affordance labels in each image. IIT-AFF also provides the bounding box of each tool, and NEDO-v1 provides accurate 3D models of the tools. However, these datasets do not have annotations about the 6DoF poses and the object class labels of each image. There are many datasets that provide the 6DoF poses of each object. The LINEMOD dataset(Hinterstoisser et al., 2012), and the T-LESS dataset(Hodaň et al., 2017) are famous datasets used for this purpose, but they dont have affordance information. There is no dataset that has annotations of multiple tasks, including affordance estimation.

2 PROPOSED DATASET

Our dataset is composed of 3D models of each tool, input scenes, and annotations.

2.1 Contents

3D Models: Our dataset provides 100 full 3D object models which captured actual objects. Table 2 shows the target objects. 10 kinds of kitchen and DIY tools with 100 instances (see Figure 2) were precisely modeled using a 3D scanner. The Solutionix C500 3D scanner from Medit Inc. was used for modeling, and mesh data comprises of roughly 500,000 vertices for each object.

Input Scene: Input scenes are the 54,867 RGB-D images of table-top situations which contain between 5 and 9 (average 6.67) target objects. Image resolution is 640×480. We randomly chosen and put objects on the table, and about 550 images of them were captured by an in-hand RGB-D camera. This procedure were repeated 100 times. We used an Intel Realsense SR305 for capturing all images. Of the images, 43,831 were for training and the rest were for testing.

Annotations: Our dataset provides four types of annotation: bounding boxes, affordance labels, object class labels, and 6DoF poses. These are labeled for all objects in the image. Bounding boxes are provided as rectangles that tightly surround the objects. Affordance labels are pixel-wise information that represent functionally of partial region on the object surface. Table 3 shows the definition of 10 labels (9 classes + background). This definition is same as that of the paper (Akizuki and Hashimoto, 2019). Object class labels are pixel-wise information that represent the object category. Eleven labels (10 classes in Table 2 + background) were prepared. A 6DoF pose, $\mathbf{T} = [\mathbf{R}, \mathbf{t}; \mathbf{0}, 1]$, represents the object pose in the input image. $\mathbf{R}$ is a 3×3 rotation matrix, and $\mathbf{t}$ is a 3×1 translation vector. 6DoF pose of all target objects are provided.

Affordance label 3D model of each target object are also assigned as color of mesh.

2.2 Statistics

Figure 3 shows the statistics of our dataset. Figure 3(a) shows the number of appearances of each object class in the scene, which is composed of 100 object layouts in total. The most frequently appeared object class, ladle, appeared 93 times, and the least frequent, hammer, appeared 40 times. The number of frequencies is in proportion to the number of objects for each class, which is explained in Table 2.

Figure 3(a) and (b) shows the distribution of affordance labels and object class labels. Note that the label background, which is assigned to other regions in the image, is ignored in this figure because the frequency is too higher compared to other classes. In figure 3(b), frequency of the label grasp is relatively higher than that of others because this label is common for all objects. The label pound is the least frequent because it is only assigned to the head part of the hammer. The distribution of the object class label shown in figure 3(c) represents the area of each object class. Therefore, the frequency of large objects became higher.

Table 1: List of RGB-D datasets that can be used for evaluating multiple tasks. Due to space limitation, some following abbreviations are used. (BBox: Bounding box, Aff mask: Affordance mask, Obj mask: Object class mask, Pose: 6DoF pose)

	Data		Annotation			
	# images	# models	BBox	Aff mask	Obj mask	Pose
RGB-D Part Affordance Dataset	31k	–	–	✓	–	–
IIT-AFF	9k	–	✓	✓	–	–
NEDO-v1	10k	72	–	✓	–	–
LINEMOD	18k	15	–	–	–	✓
T-LESS	49k	30	–	–	–	✓
Ours	54k	100	✓	✓	✓	✓

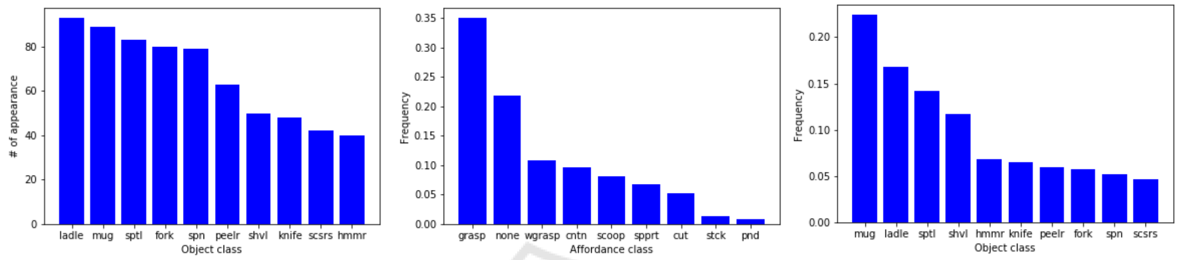

(a) Object class wise number of appearances

(b) Affordance label distribution

(c) Object class label distribution

Figure 3: Dataset statistics. Some class names are abbreviated. (sptl: spatula, spn: spoon, peelr: peeler, shvl: shovel, scsrs: scissors, hmmr: hammer, wgrasp: wrap-grasp, cntn: contain, spprt: support, stck: stick, pnd: pound.)

Table 2: Object class and the number of 3D models.

Kitchen tool	Fork(11), Knife(6), Ladle(20), Mug(15), Peeler(9), Spatula(13), Spoon(12)
DIY tool	Hammer(4), Scissors(4), Shovel(6)

Table 3: Affordance labels and corresponding colors.

Affordance	Functionality	Color
Contain	With deep cavities to hold liquid.	(255,255,0)
Cut	Used for separating another object.	(255,0,0)
Grasp	Can be enclosed by a hand.	(0,255,0)
Pound	Used for striking other objects.	(160, 160, 160)
Scoop	A curved surface that gathers soft material.	(0, 255, 255)
Stick	Sharp parts that can be pushed into something.	(0,150,0)
Support	Flat parts that can hold loose material.	(255,0,255)
Wrap-grasp	Can be held with the hand and palm.	(0,0,255)
None	Other region on objects.	(255,255,255)
Background	Other region outside of objects.	(0,0,0)

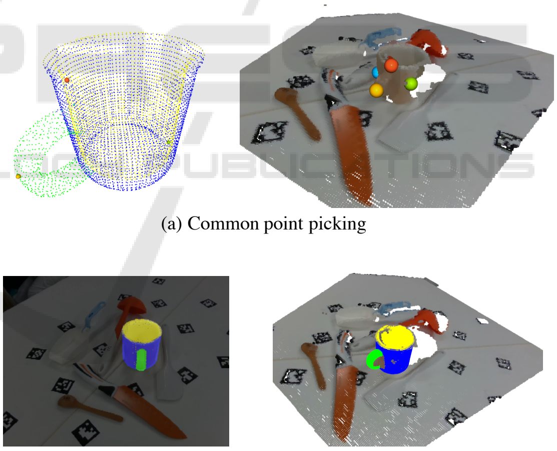

(a) Common point picking

(b) Pose refinement by ICP

(c) Annotation result

Figure 4: The annotation procedure for 6DoF pose by the developed software.

3 ANNOTATION PROCEDURE

We used a low-cost annotation procedure (Akizuki and Hashimoto, 2019) and enhanced it to generate multi-type annotations for preparing our dataset. This method allows a semi-automatic process to generate ground-truth images with pixel-wise annotations for input images taken from multiple viewpoints. The algorithm consists of three steps, as explained below.

1. 6DoF pose annotation
2. Camera pose estimation using ArUco(Garrido-Jurado et al., 2014)
3. Ground truth image rendering

In Step 1, the pose of each object in a reference image is manually estimated. We have developed a software that enables rapid annotation compared to that proposed by (Akizuki and Hashimoto, 2019). Figure 4 shows an interactive annotation procedure using our software. At first, a user picks more than three corresponding points from an object model $M_i, i = \{1, \ldots, n\}$ and a reference image I; these are displayed on screen by point cloud representation. The picked points are shown in 4(a) as colored small spheres. The software calculates the rigid transformation that aligns the object model to the input scene by aligning the picked points and renders a transformed object model on to the input scene as an image representation. Users refines the transformation using an ICP algorithm (Besl and McKay, 1992) by pressing the key, as shown in 4(b). The final transformation $\mathbf{T}_i^M = [\mathbf{R}, \mathbf{t}; \mathbf{0}, 1]$ can be checked via the 3D point cloud viewer as shown in figure 4(c).

In Step 2, relative camera poses $\mathbf{T}_j^C$ between the reference image I and the rest of the frames $I_j, j = \{1, ..., n\}$ are calculated by using ArUco library, which can accurately compute the pose of the Augmented Reality (AR) markers.

Finally, in Step 3, multiple ground-truth annotations (including bounding boxes, 6DoF poses, affordance labels, and object class labels) are generated based on the pose data computed in Steps 1 and 2. According to the results of Steps 1 and 2, the pose of the object M_i in I_n can be denoted by $\mathbf{T}_j^C \mathbf{T}_i^M$. However, the two transformations may include slight errors that should be corrected. The object models appearing in the scene M_i are merged into a point cloud after applying the transformation $\mathbf{T}_j^C \mathbf{T}_i^M$. A transformation for correction $\mathbf{T}_r$ that minimizes errors between the merged point cloud and the scene I_j is calculated by an ICP algorithm. Therefore, the final transformation is denoted by $\mathbf{T}_r \mathbf{T}_j^C \mathbf{T}_i^M$, and is applied for all object models M_i.

Annotations are generated by rendering them to the images of I_j. As for the affordance and object class labels, an assigned label of each point of M_i is rendered. Bounding boxes are calculated from the silhouettes of each model. The 6DoF poses of each model M_i in an image I_n is $\mathbf{T}_r \mathbf{T}_j^C \mathbf{T}_i^M$.

4 EXPERIMENTS

4.1 Annotation Cost

This section discusses the annotation cost of the proposed annotation software. One importance difference from the previous method (Akizuki and Hashimoto, 2019) is Step 1, the 6DoF annotation shown in figure 4(a). The previous method incrementally transformed the object model via keyboard and mouse operation. Our method only needs a few corresponding points to be picked from an object model and input scene. It is confirmed that the annotation cost of this process improved from 15–20 min to 8 min.

4.2 Object Recognition Task: Setting

We have conducted the benchmarking for our dataset using modern object recognition algorithms. Three tasks–affordance segmentation, object class segmentation and object detection–were tested. The dataset was split into a training set and a testing set. Of the 100 layouts, 80 were used as a training set and 20 were used as a testing set. Each set has 43831 and 11036 images, respectively.

4.3 Task 1: Affordance Segmentation

In this experiment, we employed the following segmentation models for comparison.

1. Fully convolutional networks (FCN-8s) (Long et al., 2015)
2. SegNet(Badrinarayanan et al., 2017)
3. Full-resolution residual networks (FRRN-A (Pohlen et al., 2017)

We trained each model for 150k iterations at a batch size of 1. To evaluate recognition performance, we used intersection over union (IoU), which is widely used as an index for segmentation tasks. IoU scores of each method are shown in Table 4. Figure5 shows the result of affordance segmentation.

Mean IoU score of FRRN-A achieved a higher score than that of others. IoU scores of affordance class that have high frequency in figure 3(b) are relatively higher compared with that of the other class. This was the common tendency of three network models.

4.4 Task 2: Object Class Segmentation

In this experiment, we used the same algorithms that were used for Task 1. IoU scores of each method are shown in Table 5. The classes mug and shovel were composed of the affordances contain, grasp, and wrap-grasp, and the IoU scores of these affordance labels were relatively higher in the Task 1 experiment. Therefore, it seems that the recognition performance of two kinds of label have a correlation.

4.5 Task 3: Object Detection

In this experiment, we evaluated the performance of object-detection tasks by comparing mean average precision (mAP) scores for each object class. We used SSD (Liu et al., 2016) for this experiment. mAP scores of each object class are shown in Table 6.

Table 4: IoU score of each affordance segmentation.

	Cntain	Cut	Grasp	Pound	Scoop	Stick	Support	Wrap-grasp	None	BG	Mean
FCN-8s	0.86	0.47	0.62	0.62	0.55	0.40	0.50	0.77	0.50	0.96	0.63
SegNet	0.62	0.42	0.62	0.33	0.47	0.31	0.00	0.76	0.44	0.96	0.49
FRRN-A	0.88	0.60	0.68	0.67	0.65	0.43	0.54	0.83	0.54	0.96	0.68

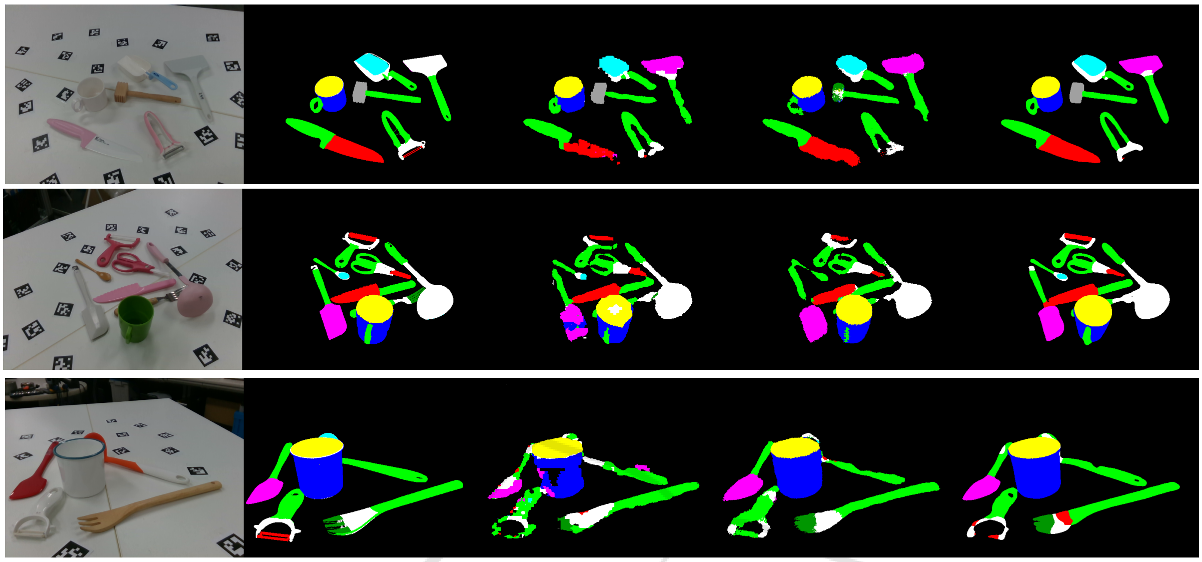

(a) Input image (b) Ground truth (c) FCN-8s (d) SegNet (e) FRRN-A

Figure 5: Result of affordance segmentation.

Table 5: IoU scores of object class segmentation.

	Fork	Knife	Ladle	Mug	Peeler	Spatula	Spoon	Hammer	Scissors	Shovel	BG	Mean
FCN-8s	0.49	0.61	0.67	0.87	0.56	0.64	0.65	0.60	0.62	0.77	0.96	0.68
SegNet	0.00	0.58	0.66	0.88	0.00	0.64	0.00	0.00	0.00	0.76	0.93	0.40
FRRN-A	0.41	0.61	0.53	0.90	0.52	0.63	0.50	0.49	0.50	0.77	0.96	0.62

Figure6 shows the result of object class segmentation. It was confirmed that mAP scores of the slender objects (spoon, fork and hammer) were relatively lower than that of other objects.

5 CONCLUSION

We have proposed a novel dataset for evaluating multiple robot vision tasks including object detection, affordance segmentation, object class segmentation, and 6DoF pose estimation. The dataset contained full 3D scans of 100 object models, 54k RGB-D scenes and annotation for four kinds of tasks. Our dataset is the largest that can be evaluated for multiple tasks, including affordance segmentation, and it is enabled to train the deep-learning architectures. We have reported the benchmarking results of affordance segmentation, object class segmentation, and object detection. In the near future, we will expand the number of deep-learning architectures for benchmarking and will perform the benchmarking of 6DoF pose estimation.

REFERENCES

Akizuki, S. and Hashimoto, M. (2019). Semi-automatic training data generation for semantic segmentation using 6dof pose estimation. In *International Joint Conference on Computer Vision, Imaging and Computer Graphics Theory and Applications(VISAPP)*.

Badrinarayanan, V., Kendall, A., and Cipolla, R. (2017). Segnet: A deep convolutional encoder-decoder architecture for image segmentation. *IEEE Transactions on Pattern Analysis and Machine Intelligence*.

Besl, P. and McKay, N. (1992). A Method for Registration of 3-D Shapes. *IEEE Transactions on Pattern Analysis and Machine Intelligence (PAMI)*, 14(2):239–256.

Do, T.-T., Nguyen, A., and Reid, I. (2018). Affordancenet: An end-to-end deep learning approach for object af-

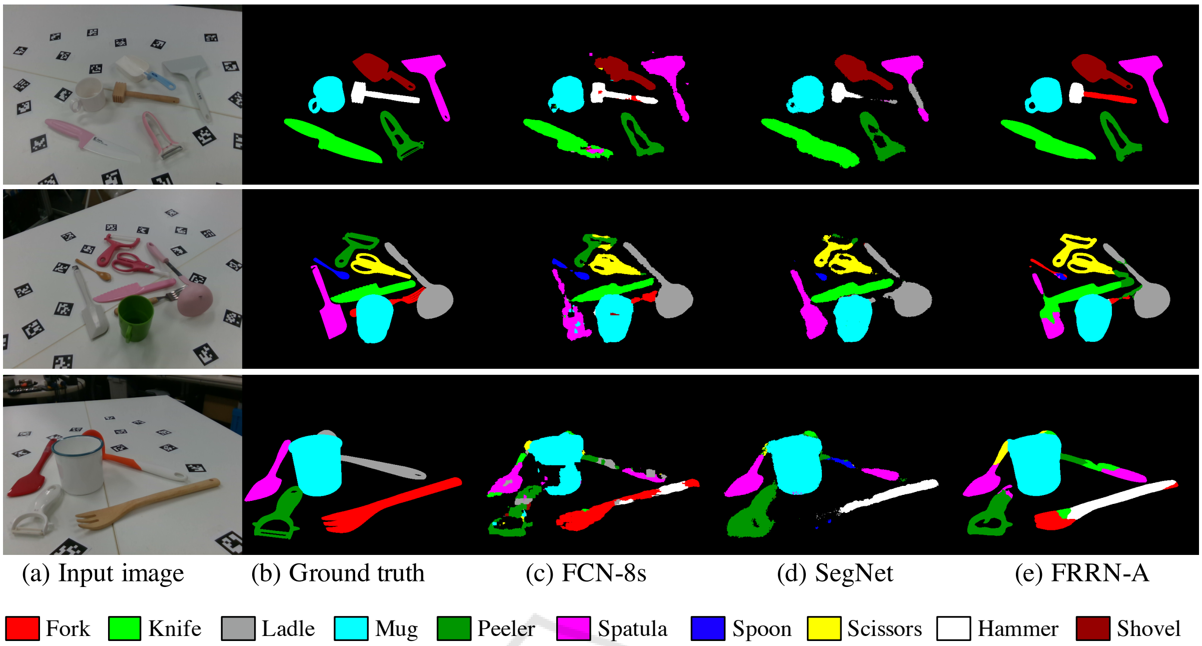

(a) Input image (b) Ground truth (c) FCN-8s (d) SegNet (e) FRRN-A

(f) Object class label

Figure 6: Result of object class segmentation.

Table 6: mAP scores of object detection.

	Fork	Knife	Ladle	Mug	Peeler	Spatula	Spoon	Hammer	Scissors	Shovel	Mean
SSD	0.75	0.84	0.88	0.91	0.88	0.85	0.78	0.79	0.89	0.88	0.84

fordance detection. In *International Conference on Robotics and Automation (ICRA)*.

Garrido-Jurado, S., Muñoz Salinas, R., Madrid-Cuevas, F., and Marín-Jiménez, M. (2014). Automatic generation and detection of highly reliable fiducial markers under occlusion. *Pattern Recognition*, 47(6):2280–2292.

Hinterstoisser, S., Cagniart, C., Ilic, S., Sturm, P., Navab, N., Fua, P., and Lepetit, V. (2012). Gradient response maps for real-time detection of texture-less objects. *IEEE Transactions on Pattern Analysis and Machine Intelligence*.

Hodaň, T., Haluza, P., Obdržálek, Š., Matas, J., Lourakis, M., and Zabulis, X. (2017). T-LESS: An RGB-D dataset for 6D pose estimation of texture-less objects. *IEEE Winter Conference on Applications of Computer Vision (WACV)*.

Liu, W., Anguelov, D., Erhan, D., Szegedy, C., Reed, S., Fu, C.-Y., and Berg, A. C. (2016). Ssd: Single shot multibox detector. In *European conference on computer vision (ECCV)*, pages 21–37. Springer.

Long, J., Shelhamer, E., and Darrell, T. (2015). Fully convolutional networks for semantic segmentation. In *Proceedings of the IEEE conference on computer vision and pattern recognition*, pages 3431–3440.

Mahler, J., Matl, M., Satish, V., Danielczuk, M., DeRose, B., McKinley, S., and Goldberg, K. (2019). Learning ambidextrous robot grasping policies. *Science Robotics*, 4(26):eaau4984.

Myers, A., Teo, C. L., Fermüller, C., and Aloimonos, Y. (2015). Affordance detection of tool parts from geometric features. In *International Conference on Robotics and Automation (ICRA)*, pages 1374–1381.

Pohlen, T., Hermans, A., Mathias, M., and Leibe, B. (2017). Full-resolution residual networks for semantic segmentation in street scenes. In *IEEE Conference on Computer Vision and Pattern Recognition (CVPR)*.